

Ab Initio Studies on the Thermal Dissociation Channels of *cis*- and *trans*-Azomethane

Nicole W. C. Hon,[†] Zhi-Da Chen,^{†,‡} and Zhi-Feng Liu^{*,†}

Department of Chemistry, The Chinese University of Hong Kong, Shatin, Hong Kong, China, and
Department of Chemistry, Peking University, Beijing, 100871, China

Received: September 5, 2001; In Final Form: April 16, 2002

The unimolecular dissociation of azomethane is studied by first sampling the reaction channels with a density functional theory based ab initio molecular dynamics method and then by mapping out the reaction barrier and transition structure for each channel with Gaussian based ab initio method at G3 and B3LYP/6-31G(d) levels. A number of new dissociation channels are identified, and all of them involve the migration of H atoms or the breaking of a C–H bond. There is also notable difference among these channels for *trans*- and *cis*-azomethane. In the gas phase, a CH₄ loss channel could be present in the dissociation of *cis*-azomethane. For N–N bond cleavage observed on metal surfaces, the hydrogen migration from C to N atoms, by either 1,2- or 1,3-hydrogen shifts, is the first step. Further H migration could result in N–N cleavage and produce HCN and CH₃NH₂, both observed in previous surface experiments. The concerted C–H bond cleavages in *cis*-azomethane could also produce H₂.

Introduction

The dissociation of azomethane, CH₃NNCH₃, has long been used as a source of methyl groups,^{1,2} while in recent years there have been renewed interests in the dynamics and mechanisms underlying such a dissociation process, both in the gas phase and on metal surfaces. In the gas phase, the focus has been on the cleavage of the two C–N bonds: whether it is “stepwise”^{3–5} or “concerted”.⁶ Although the semantics of those terms is not uniform among different authors,^{6,7} recent experiments all seemed to point to a very short time lag (~1 ps) between the breaking of the two C–N bonds.^{6–9} This problem has also been studied in great detail by theoretical calculations. Although a transition state for simultaneous C–N bond cleavage was identified,¹⁰ there is a consensus that the sequential mechanism is more important than the simultaneous cleavage.^{10,11} The product •CH₃N₂ radical after the initial dissociation step was found to be highly unstable with a very low dissociation barrier around 2.3 kcal/mol.^{12,13} Coupled with the considerable thermal energy deposited in azomethane during the photoexcitation process, it accounted for the experimental observation of a short time delay (~1 ps) between the two cleavage steps.^{10–12} This conclusion was further supported by a semiclassical dynamics study on the C–N cleavages¹⁴ based on ab initio fitted potential energy surfaces.¹⁵

On metal surfaces,^{16–21} the dissociation of azomethane is much more complicated than that in the gas phase. Although part of the motivation for such studies is to find a way to produce adsorbed methyl groups, the C–N cleavage plays only a minor role in the dissociation. Both *cis*^{18,19} and *trans*^{16,17} isomers of CH₃NNCH₃ were observed on surfaces, and transformation from *trans* to *cis* could proceed at low temperature around 100 K.^{18,19} The N–N cleavage, instead of C–N cleavage, was most often observed,^{16,17,19,21} which could be preceded by a hydrogen migration step to form CH₃NHN=CH₂, formaldehyde methyl-

hydrazone.^{16,18,19} The final products of dissociation could include C₂N₂, H₂, N₂, HCN, CH₃NH₂, and CH₄, depending on experimental conditions.

The *trans* isomer of azomethane is more stable than its *cis* isomer, and transformation between the two isomers has also been studied in great detail by theoretical calculations.^{10,22–26} As mentioned above, both isomers make a contribution to the dissociation on metal surfaces. In the gas phase, the *trans* isomer should dominate. However, the dissociation of azomethane in gas-phase studies are usually initiated by UV photoexcitation. The crossing point from the excited S₁ state to the S₀ ground state was identified by high level ab initio calculations as an asymmetrical structure with a CNNC dihedral angle of 92.81°.¹⁰ This rotation of the N–N bond prior to internal conversion indicates that both the *trans* and *cis* isomers should be present in the gas-phase experiment,⁶ although little attention has been paid to the possible difference between the dissociation of *cis*- and *trans*-azomethane. Furthermore, the complexity of the azomethane dissociation on surfaces seems to indicate that there may well be other dissociation or isomerization channels, which are probably catalyzed by metal surfaces. Thus, in addition to the works reported on the C–N cleavage and *cis*–*trans* transformation, further studies on the dissociation and isomerization channels for both *trans*- and *cis*-azomethane would be desirable for designing a suitable potential energy surface in dynamics studies, for understanding the finer details in gas-phase experiments, and for identifying the processes catalyzed by metal surfaces.

In this paper, we report a computational study to explore these other reaction channels on the ground-state potential surfaces for both *trans*- and *cis*-azomethane.

Computational Details

The trajectories of unimolecular dissociation of CH₃NNCH₃ were sampled by the VASP program (Vienna *Ab-Initio* Simulation Package), developed at the Institut für Theoretische Physik of the Technische Universität Wien.^{27–30} The principles of the

* Corresponding author: zfliu@cuhk.edu.hk

[†] The Chinese University of Hong Kong.

[‡] Peking University.

ab initio molecular dynamics (AIMD) method have been documented in the literature^{31–35} and will not be reproduced here. The molecule was put in a periodic cubic box with a length of 12 Å, so that there is little interaction between molecules in neighboring cells. A planewave basis set with a cutoff energy of 225 eV was employed for the wave function, which was solved at each AIMD step by conjugate gradient minimization of the total electronic energy within the framework of the generalized gradient approximation (GGA)³⁶ for density functional theory. The core region of an atom was approximated by the Vanderbilt³⁷ ultrasoft pseudopotentials supplied with the VASP package.^{38,39} Only Γ point was considered for k-point sampling.

For *cis*- and *trans*-azomethane, one hundred trajectories were run for each molecule. With our purpose limited to the sampling of reaction channels without resorting to any empirical assumptions, we adopted a simplified and straightforward procedure for the AIMD simulations. A preliminary equilibration simulation was performed at 2000 K, starting with the equilibrium azomethane geometry in the ground state, for a duration of 10 ps with a 0.5 fs time step. One hundred geometric configurations were randomly selected from the equilibration run as starting geometries for the trajectory study, while initial velocities were also randomly selected according to a Boltzmann distribution determined by the simulation temperature.

For each trajectory, the duration of simulation was set at 3 ps (6000 steps with a 0.5 fs time step), and the system was controlled by a Nosé-Hoover thermostat^{40,41} at a temperature of 3500 K, corresponding to an average thermal energy of 3.6 eV. The total translation and rotation of the simulated molecule were set to zero at each time step during the simulation.

After the sampling of reaction channels by AIMD simulations, each channel is further studied by Gaussian based methods to map out the transition structure and energy barrier. Such an approach of combining AIMD simulations with Gaussian based methods to study the unimolecular dissociation reactions has been successfully applied before by our group.^{42,43} For this study, transition structures were optimized at the G3 level⁴⁴ and its variations⁴⁵ G3(MP2) and G3B3, and also at the B3LYP/6-31G(d) level, both as implemented in the GAUSSIAN 98 package.⁴⁶ The G3 method offers a good compromise between accuracy and computational cost, as shown in the test for a wide range of organic molecules.⁴⁴ The G3 results are further compared with density functional theory calculations, using the B3LYP functional with a 6-31G(d) basis set. B3LYP has been widely used for the study of reaction barriers and has proved to be a fairly accurate method,⁴⁷ thus offering a corroboration of the G3 results. As will be discussed in the next section, additional calculations were also performed with a larger basis set of 6-311G(2d,p) and at CASSCF/MCSCF levels to further check and verify the quality of our calculations.

Results and Discussion

The reaction channels found in the AIMD trajectories for *trans*- and *cis*-azomethane are listed in Tables 1 and 2, together with the energy barriers located by the Gaussian-based G3, G3B3, G3(MP2), and B3LYP/6-31G(d) methods. These channels could be broadly divided into two categories. The first involves the breaking of the C–N and N–N bonds, as in the dissociation and isomerization channels. The rest of the channels all involve H atoms, and the breaking of C–H bonds.

Dissociation and Isomerization Channels. Since extensive theoretical studies on the dissociation and isomerization processes have been reported before,^{10–15} the reaction barriers for

these processes could be taken as a calibration for the methods used in this study. Overall, there is excellent agreement between the G3 and the B3LYP/6-31G(d) results, and both are also in good agreement with previously reported values. We did notice some spin contamination ($S^2 = 0.1–0.2$) in the G3 optimized transition structures for the 1,2-hydrogen shift process, as it was performed at the UHF/6-31G(d) level. However, there is no spin contamination for the B3LYP/6-31G(d) results. Additional calculations were also performed at the QCISD(T)//MP2/6-311G(2d,p) level to verify the reaction barriers reported in Tables 1 and 2 and that the obtained values were within 2 kcal/mol of the G3 values. The verification calculations indicate that the 6-31G(d) basis set used in both our G3 and B3LYP calculations are quite adequate. In the following discussions, the calculated energy and geometrical parameters are values at the G3 level unless otherwise explicitly specified.

For *trans*-to-*cis* isomerization, there are two reaction pathways suggested in previous reports.^{22–26} In a rotational pathway, the dihedral angle CNNC is changed from 180° to 0° with the methyl group moving to the other side by rotating out of the plane of the N=N double bond, while in a semi-linearization pathway, the CNN angle is changed from 120° to 240° with the methyl group staying within the N=N plane. At the G3 level, our calculated energy barrier is 50.8 kcal/mol for the rotational pathway, compared to 49.5 kcal/mol by CASPT2 results.²⁵ For the semi-linearization path, the barrier is 53.6 kcal/mol, compared to the CASPT2 result of 54.2 kcal/mol.²⁵

For the C–N bond cleavage, the energy required for stepwise dissociation is found to be 51.3 kcal/mol for *trans*-azomethane and 42.1 kcal/mol for *cis*-azomethane (Tables 1 and 2). However, no transition structure was found at the G3 level for a concerted dissociation in *trans*-azomethane. It has been previously noted that a large basis set is needed to locate this transition structure.^{10,11} The G3 method is inadequate since its structure optimization is performed at the UHF/6-31G(d) level,⁴⁴ and the B3LYP/6-31G(d) method also did not locate such a transition structure. However, a transition structure is found when the full MP2 treatment is included in the structure optimization of G3 method, known as G3(MP2).⁴⁵ Furthermore, we have also located a transition structure for the concerted dissociation for *cis*-azomethane, again with a reaction barrier lower in energy than that for the stepwise process.¹⁰ The structure parameters of these two transition structures, **TS1–1** and **TS1–2**, are shown in Figure 1, and their N–C distances are close to each other with a difference of less than 0.01 Å. (Atomic coordinates for all of the transition and intermediate structures shown in Figures 1–5 are given as Supporting Information.)

Unfortunately, we cannot locate transition structures using the VASP program, within its framework of density functional theory with a planewave basis set and pseudopotentials. The quality of VASP calculations could be measured by the geometrical parameters for the *trans*- and *cis*-azomethane, as shown in Table 3 and by the homolysis barrier in the stepwise dissociation (Tables 1 and 2). The geometry parameters obtained in VASP calculations are in good agreement with the ab initio^{11,14} and experimental results,⁴⁸ with bond lengths slightly overestimated by the VASP calculations. The energy difference between *trans*- and *cis*-azomethane is 9.0 kcal/mol in VASP, also in good agreement with the value of 9.2 kcal/mol at both the G3 and the B3LYP/6-31G(d) levels. However, the barrier for the stepwise dissociation obtained by VASP is 66.1 kcal/mol for *trans*-azomethane and 57.1 kcal/mol for *cis*-azomethane, both being around 15 kcal/mol higher than the corresponding

TABLE 1: Reaction Barriers in the Thermal Dissociation Channels for *trans*-Azomethane Observed in AIMD Trajectory Studies

	Energy (Kcal/mol)				Frequency observed in AIMD trajectories	
	G3	G3B3	G3 MP2/ 6-31G(d)	B3LYP/ 6-31G(d) VASP		
Stepwise dissociation ^a	51.3	51.7	54.0	48.8	66.1	14
$\text{H}_3\text{C}-\text{N}=\text{N}-\text{CH}_3 \longrightarrow \text{H}_3\text{C}-\text{N}=\text{N}\cdot + \text{H}_3\text{C}\cdot \longrightarrow 2 \text{H}_3\text{C}\cdot + \text{N}\equiv\text{N}$						
Concerted dissociation ^b	45.4				13	
$\text{H}_3\text{C}-\text{N}=\text{N}-\text{CH}_3 \longrightarrow 2 \text{H}_3\text{C}\cdot + \text{N}\equiv\text{N}$						
Isomerization ^c	50.8	53.4		49.3		12
$\text{H}_3\text{C}-\text{N}=\text{N}-\text{CH}_3 \longrightarrow \text{H}_3\text{C}-\text{N}=\text{N}-\text{CH}_3$						
1,3 H shift	63.4	63.4		63.7		19
$\text{H}_3\text{C}-\text{N}=\text{N}-\text{CH}_3 \longrightarrow \text{H}_2\text{C}=\text{N}-\text{N}-\text{CH}_3$						
1,2 H shift	66.8	65.0		66.3		5
$\text{H}_3\text{C}-\text{N}=\text{N}-\text{CH}_3 \longrightarrow \text{H}_2\text{C}=\text{N}^+-\text{N}-\text{CH}_3$						
H ₂ elimination		81.1		79.4		2
$\text{H}_3\text{C}-\text{N}=\text{N}-\text{CH}_3 \longrightarrow \text{HC}^--\text{N}^+=\text{N}-\text{CH}_3 + \text{H}_2$						
H radical dissociation	87.7	87.9		83.9		1
$\text{H}_3\text{C}-\text{N}=\text{N}-\text{CH}_3 \longrightarrow \text{H}_2\text{C}\cdot-\text{N}-\text{N}-\text{CH}_3 + \text{H}\cdot$						

^a The energy is for the first C–N bond cleavage. Previously reported values are 46.3 kcal/mol at the CCSDT/TZ2P level (ref 11), 51.5 kcal/mol at the OCISDT/6-311G(2d,p) level (ref 10), and 54.7 kcal/mol at the CCSD/DZP level (ref 25). ^b Previously reported value is 44.2 kcal/mol at the QCISDT/6-311G(2d,p) level (ref 10). ^c Previously reported value is 49.5 kcal/mol at the CASPT2/DZP level (ref 25).

values obtained by the Gaussian-based methods (Tables 1 and 2), which is probably due to the pseudopotentials and the low energy cutoff for the AIMD simulations. Accordingly, the frequency for the observed stepwise dissociation is likely underestimated. It is also a reminder of the benefit to check the transition structure and energy barrier at a higher level of theory for each reaction channel observed in the AIMD trajectory study.

Indeed, the concerted dissociation is as frequent in our study as the stepwise dissociation, which is in fortuitous agreement with the trajectory study reported by Cattaneo and Persico, using a potential surface fitted to *ab initio* calculations.¹⁴ Similar to their results, we also observed a very short time lag (less than 0.5 ps) between the two dissociation steps and accordingly used their method to distinguish the two kinds of bond dissociation. It is defined as stepwise when one of the C–N bond lengths is shorter than 2.23 Å and the other one is greater than 4.5 Å; otherwise, the channel is deemed as concerted.

Methane Elimination. There are a number of new dissociation channels discovered in our AIMD trajectory study, and all of them are related to the migration of hydrogen atoms. The azomethane configuration, being *trans* or *cis*, is an important factor in such processes. Methane elimination is one of these new channels, with a hydrogen atom on one methyl group moving to the other group to form a methane molecule and leaving CH₂N₂, diazomethane, as the other fragment. A similar process was observed before in the thermal dissociation of acetic acid, in which the hydrogen atom on the hydroxy group could move to the methyl group to form methane.^{43,49–51} It is obvious that such a reaction requires the two methyl groups on the same side and could happen only for *cis*-azomethane.

The transition structure **TS1–3** for the methane elimination channel shown in Figure 1 was obtained at the B3LYP/6-31G(d) level, as the G3 method failed to locate a transition structure. The C–N distance for the departing methyl group is at 2.42 Å,

TABLE 2: Reaction Barriers in the Thermal Dissociation Channels for *cis*-Azomethane Observed in AIMD Trajectory Studies

	Energy (Kcal/mol)				Frequency observed in AIMD trajectories	
	G3	G3B3	G3 MP2/ 6- 31G(d)	B3LYP/ 6-31G(d) VASP		
Stepwise dissociation ^a $\begin{array}{c} \text{N}=\text{N} \\ \diagup \quad \diagdown \\ \text{H}_3\text{C} \quad \text{CH}_3 \end{array} \longrightarrow \begin{array}{c} \text{N}=\text{N}\cdot \\ \diagup \\ \text{H}_3\text{C} \end{array} + \text{H}_3\text{C}\cdot \longrightarrow 2 \text{H}_3\text{C}\cdot + \text{N}\equiv\text{N}$	42.1	42.5	44.8	39.6	57.1	16
Concerted dissociation $\begin{array}{c} \text{N}=\text{N} \\ \diagup \quad \diagdown \\ \text{H}_3\text{C} \quad \text{CH}_3 \end{array} \longrightarrow 2 \text{H}_3\text{C}\cdot + \text{N}\equiv\text{N}$			37.6			19
Isomerization $\begin{array}{c} \text{N}=\text{N} \\ \diagup \quad \diagdown \\ \text{H}_3\text{C} \quad \text{CH}_3 \end{array} \longrightarrow \begin{array}{c} \text{CH}_3 \\ \diagup \\ \text{N}=\text{N} \\ \diagdown \\ \text{H}_3\text{C} \end{array}$	41.6	44.2		40.1		20
CH ₄ elimination $\begin{array}{c} \text{N}=\text{N} \\ \diagup \quad \diagdown \\ \text{H}_3\text{C} \quad \text{CH}_3 \end{array} \longrightarrow \text{H}_2\text{C}=\text{N}^+\text{N}^- + \text{CH}_4$		47.9		47.5		12
1,2 H shift $\begin{array}{c} \text{N}=\text{N} \\ \diagup \quad \diagdown \\ \text{H}_3\text{C} \quad \text{CH}_3 \end{array} \longrightarrow \begin{array}{c} \text{H} \\ \diagup \\ \text{N}^+-\text{N}^- \\ \diagdown \\ \text{H}_2\text{C} \quad \text{CH}_3 \end{array}$	59.7	58.7		60.0		7
H ₂ elimination (A) $\begin{array}{c} \text{N}=\text{N} \\ \diagup \quad \diagdown \\ \text{H}_3\text{C} \quad \text{CH}_3 \end{array} \longrightarrow \begin{array}{c} \text{CH}_2 \\ \diagup \\ \text{N}=\text{N} \\ \diagdown \\ \text{H}_2\text{C} \end{array} + \text{H}_2$	57.8	59.7		58.4		3
H ₂ elimination (B) $\begin{array}{c} \text{N}=\text{N} \\ \diagup \quad \diagdown \\ \text{H}_3\text{C} \quad \text{CH}_3 \end{array} \longrightarrow \begin{array}{c} \text{HC}^- \\ \diagup \\ \text{N}^+=\text{N} \\ \diagdown \\ \text{CH}_3 \end{array} + \text{H}_2$		77.6		75.5		4

^a The energy is for the first C–N cleavage.

which is 0.2 Å longer than the C–N distance around 2.23 Å in the transition structure for the concerted C–N homolysis of *cis*-azomethane (TS1–2). Thus, both the hydrogen migration and the C–N bond breaking are involved in this reaction, and it could be viewed as a process in which a dissociating CH₃ radical captures a H atom from the remaining methyl group as it leaves. The reaction barrier is higher than that for the stepwise dissociation by 7.9 kcal/mol.

The existence of such a channel is further verified by complete active space self-consistent-field (CASSCF) calculations with the active space of (10,8), including the bonding and antibonding π orbitals, the two lone pairs on nitrogen atoms, and the two pairs of C–N σ bonding and antibonding orbitals, and using the same basis set 6-31G(d). A transition structure was located and it differed from TS1–3 in that the N1–C3 distance was further increased to a value of 3.6 Å, which is consistent with the interpretation of this channel as a departing methyl group picking up a hydrogen atom from the other methyl group.

A significant number of trajectories are observed in the AIMD simulation for this channel (Table 2), although it is only a qualitative estimate as the total number of trajectories is small. To further explore the rate of CH₄ elimination versus the rate for homolysis, we also performed RRKM calculations^{52,53} using the reaction barriers, vibrational frequencies, and structure parameters obtained at the B3LYP/6-31G(d) level. Above 2000 K, the rate constant for the CH₄ elimination channel is more than one-fifth of the rate constant for stepwise homolysis.

It should be noted that unimolecular dissociation initiated by UV excitation is not the same as the thermal dissociation in our study. However, in previous experiments^{6,8} it has been found that for the slow CH₃ group due to the first C–N homolysis, the translation energy is peaked at 4 kcal/mol⁶ and the vibrational energy is averaged around 8.2 kcal/mol.⁸ Without even considering the internal energy in the other methyl group, this amount of energy is already enough to compensate for the 7.9 kcal/mol difference between the barriers of CH₄ elimination and stepwise homolysis at the B3LYP/6-31G(d) level. Due to

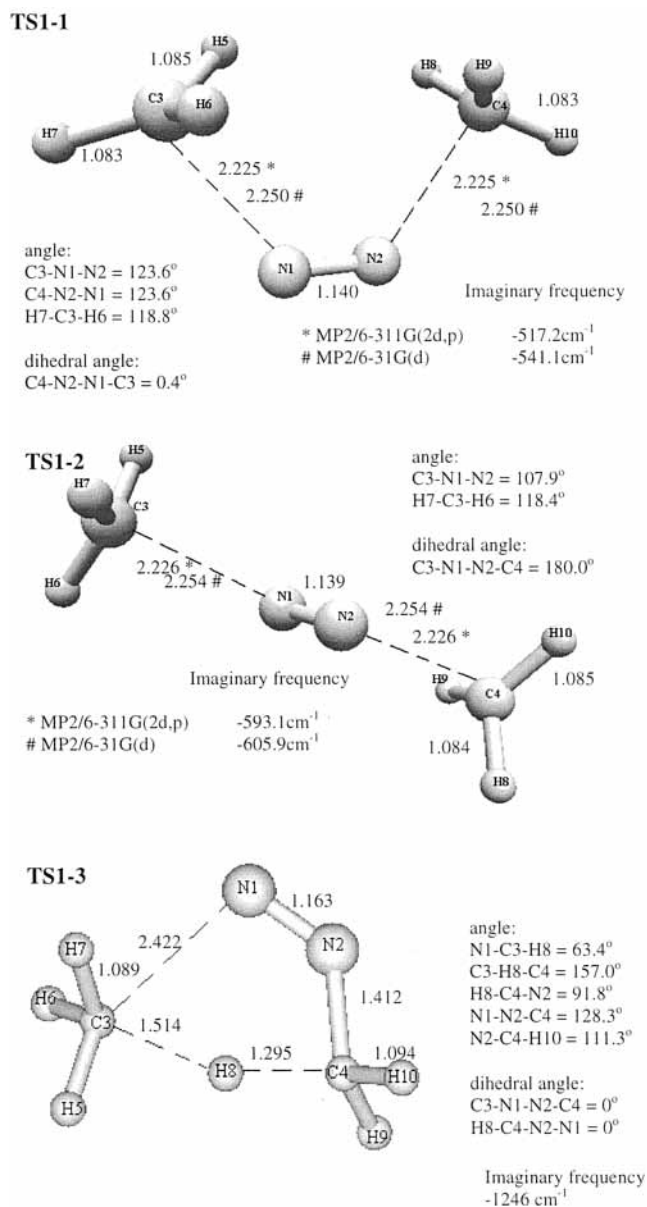


Figure 1. Transition structures for the concerted dissociation in *trans*- and *cis*-azomethane (**TS1-1** and **TS1-2**) and for the methane elimination (**TS1-3**) at the B3LYP/6-31G(d) level. Bond distances are in Å. Notice the C3-N1 distance in **TS1-3** is 2.435 Å, 0.2 Å longer than the N-C distances in **TS1-1** and **TS1-2**. It indicates that C3-N1 bond is almost broken when the departing methyl group captures a hydrogen atom from the other methyl group. Such a channel requires the two methyl group being at the same side of the N=N bond and is open only to *cis*-azomethane.

the large amount of energy deposited in azomethane after UV excitation, it is quite likely that the departing CH₃ group could pick up a H atom from the other CH₃ group, as in the thermal dissociation, when the two fragments are properly oriented.

The presence of this channel will also depend on the amount of *cis*-azomethane in the sample. For thermal dissociation, reaction rate calculations indicated that the isomerization between *trans*- and *cis*-azomethane would be overshadowed by the C-N bond homolysis and there would be little *cis*-azomethane.²⁵ However, in the photoexcitation experiments, the crossing point between the excited state and the ground state was found to be asymmetrical with a CNNC dihedral angle of 92.8°,¹⁰ implying a significant amount of *cis*-azomethane. Accordingly, although the dissociation in gas phase should be

dominated by the C-N bond homolysis, the presence of the CH₄ elimination channel cannot be ruled out. In that case, the intensity of CH₄ signal or the lack of it could be potentially used as a measure of the abundance of *cis*-azomethane in future experiments. Interestingly, the other product in the CH₄ elimination channel, diazomethane (CH₂N₂), is a well-known source of methylene, CH₂. A significant number of signals with *m/e* = 14 (CH₂⁺) was detected in a previous molecular beam experiment, although it was attributed to N⁺ or N₂²⁺ contamination.⁶

Hydrogen Shift Channels and N-N Bond Cleavage. Hydrogen shift from the methyl group to the nitrogen atoms in azomethane was observed in several experimental studies on metal surfaces, for both *cis*^{18,19} and *trans*-azomethane.¹⁶ The process could be initiated either by UV irradiation¹⁶ or simply by thermal heating,^{18,19} while the product was identified as formaldehyde methylhydrazone, CH₃NHN=CH₂. Synthesis of this compound was reported before.⁵⁴ Not much was known about its structure, except for the geometrical parameters obtained by ab initio calculations.⁵⁵ It was also claimed that *cis*-azomethane was quite reactive in the gas phase and readily isomerized into CH₃NHN=CH₂ even at room temperature, although little data was presented for the identification of this process.⁵⁶

Our AIMD trajectory study identified more than one type of hydrogen shift channel (Tables 1 and 2). As shown in Figure 2, both 1,2- (see **2-1**) and 1,3-hydrogen shifts (see **2-2**) are possible for *trans*-azomethane, while for the *cis*-azomethane, the 1,3-hydrogen shift is blocked by the steric repulsion of the other methyl group, and only the 1,2-hydrogen shift (see **2-3**) is observed. Structure parameters obtained for **2-2**, the *trans*-formaldehyde methylhydrazone formed in the 1,3-hydrogen shift of *trans*-azomethane, are in good agreement with previous results.⁵⁵ The energy loss in this process is fairly small, 3.2 kcal/mol, compared to around 6 kcal/mol at the MP4/6-31G* level.⁵⁵ Structure **2-2** is also 21.6 kcal/mol more stable than **2-1**, the product of 1,2-hydrogen shift, in which there is charge separation on the two nitrogen atoms. However, the N-N distance in **2-1** at 1.301 Å is shorter than the distance of 1.377 Å in **2-2**. The CNNC dihedral angle in **2-1** is 173.2°, indicating a degree of double bonding between the two nitrogen atoms. The N-N bonding in **2-1** is thus stronger than that in **2-2**.

Transition structures for these reactions are shown in Figure 3. For *trans*-azomethane, the barrier height for the 1,3-hydrogen shift is only 3.4 kcal/mol lower than that for the 1,2-hydrogen shift. Although a direct 1,3-hydrogen shift is inaccessible in *cis*-azomethane, further H migration (2,3-hydrogen shift) is possible for **2-3**, the product of 1,2-hydrogen shift, to form *cis*-formaldehyde methylhydrazone (**2-4**) through the transition structure **TS3-4**, and the energy barrier of 40.9 kcal/mol at G3 level and of 43.1 kcal/mol at B3LYP/6-31G(d) level is lower than that for the initial 1,2-hydrogen shift at 59.7 kcal/mol. Structure **2-4** is 17.3 kcal/mol more stable than **2-3**. A similar 2,3-hydrogen shift process is also possible for the isomerization of **2-1** into **2-2** with a barrier of 49.0 kcal/mol at G3 level and 50.4 kcal/mol at B3LYP/6-31G(d). It should also be noted that spin contamination in G3 calculations was again observed in the transition structures for the 2,3-hydrogen shift reactions, but the energy barriers calculated were nonetheless in good agreement with the B3LYP/6-31G(d) values, which showed no spin contamination at all.

Structures **2-3** and **2-1** are *cis-trans* isomers, with **2-1** being 4.5 kcal/mol less stable than **2-3**. The barrier for rotation around the N-N bond is 48.5 kcal/mol, again indicating a double bond

TABLE 3: Equilibrium Geometrical Parameters for Ground-State *cis*- and *trans*-Azomethane with Bond Distances in Å and Angles in Degrees

	VASP	G3	MP2/6-311G(2d,2p)	B3LYP/6-31g(d)	TZ2P/SCF ^a	TZ2P/CISD ^a	CASSCF ^b	expt
trans								
R_{NN}	1.334	1.212	1.253	1.244	1.204	1.220	1.255	1.247
R_{CN}	1.485	1.454	1.465	1.467	1.453	1.458	1.467	1.482
R_{CH}	1.104	1.083	1.092	1.096	1.081	1.081	1.105	1.105
$\angle NNC$	111.4	113.7	111.7	112.5	114.1	113.1	112.4	112.3
cis								
R_{NN}	1.330	1.215	1.255	1.243	1.208	1.224	1.257	
R_{CN}	1.498	1.465	1.478	1.484	1.464	1.470	1.463	
R_{CH}	1.100	1.080	1.082	1.091	1.077	1.077		
$\angle NNC$	118.7	120.7	118.8	120.0	120.6	119.0	124.3	

^a Reference 11. ^b Reference 14. ^c Reference 47.

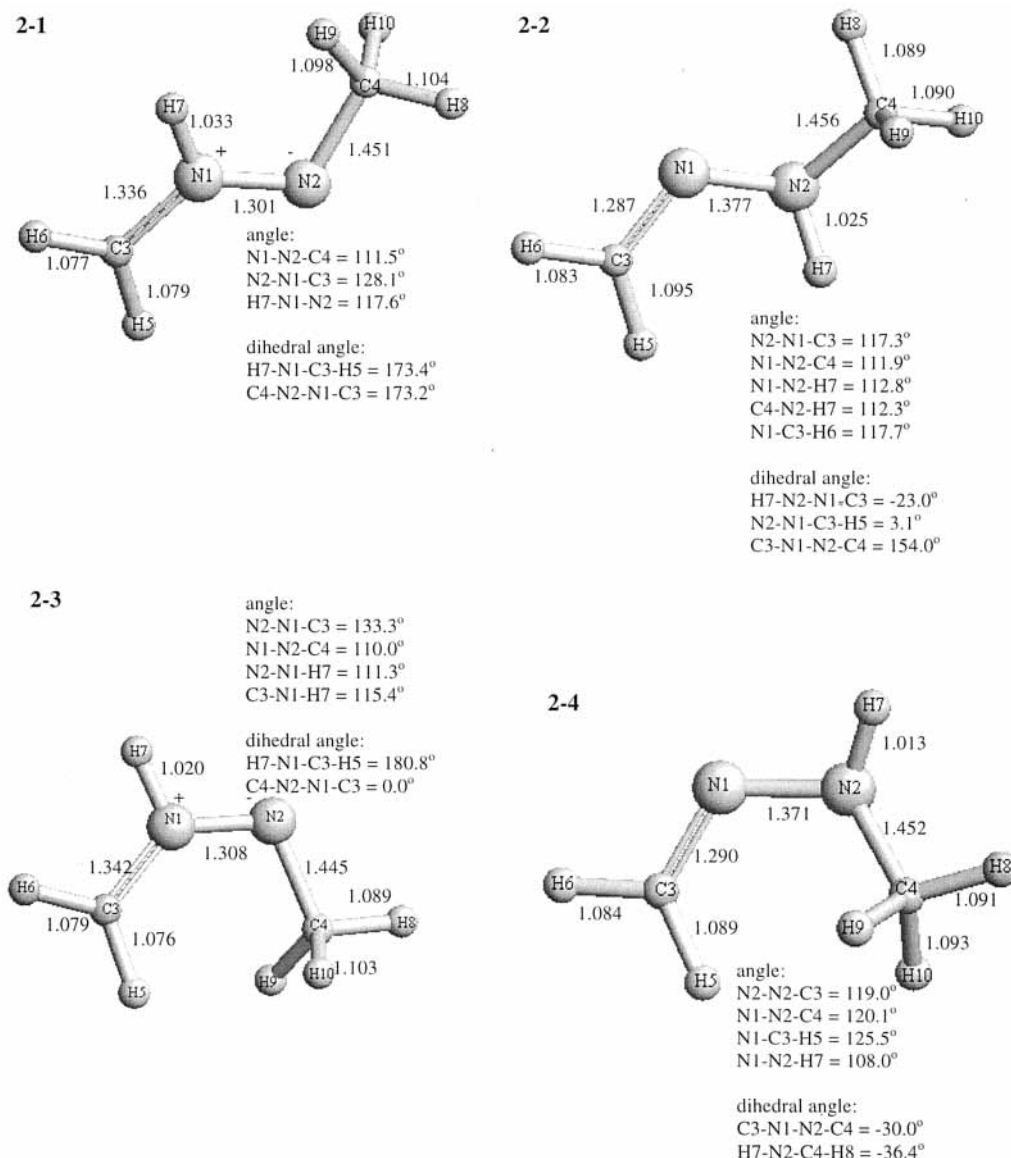


Figure 2. The optimized structures at G3 level for the products of 1,2- and 1,3-hydrogen shifts. Bond distances are in Å. The CNNC dihedral angles in 2-1 and 2-3 are close to either 180° or 0°, indicating a degree of N-N double bond. A direct route for the 1,3-hydrogen shift for *cis*-azomethane to produce 2-4 is not accessible because of the steric repulsion of the methyl group. Instead, 2-4 is produced by a further H migration in 2-3.

between the two N atoms in 2-1 and 2-3. In contrast, the energy difference between 2-2 and 2-4 is only 0.2 kcal/mol, with the former being less stable, while the N-N rotation barrier is only 4.7 kcal/mol.

Compared to the C-N bond cleavage channels, the reaction barriers for H migration from carbon to nitrogen atoms are more

than 12 kcal/mol higher. That these channels become more important for azomethane adsorbed on metal surfaces is probably due to the weakening of C-H bond upon adsorption and the channeling of photoexcitation or thermal excitation energy into the C-H bending and stretching vibrations in the methyl groups. The claim that gas-phase *cis*-azomethane could readily isomerize

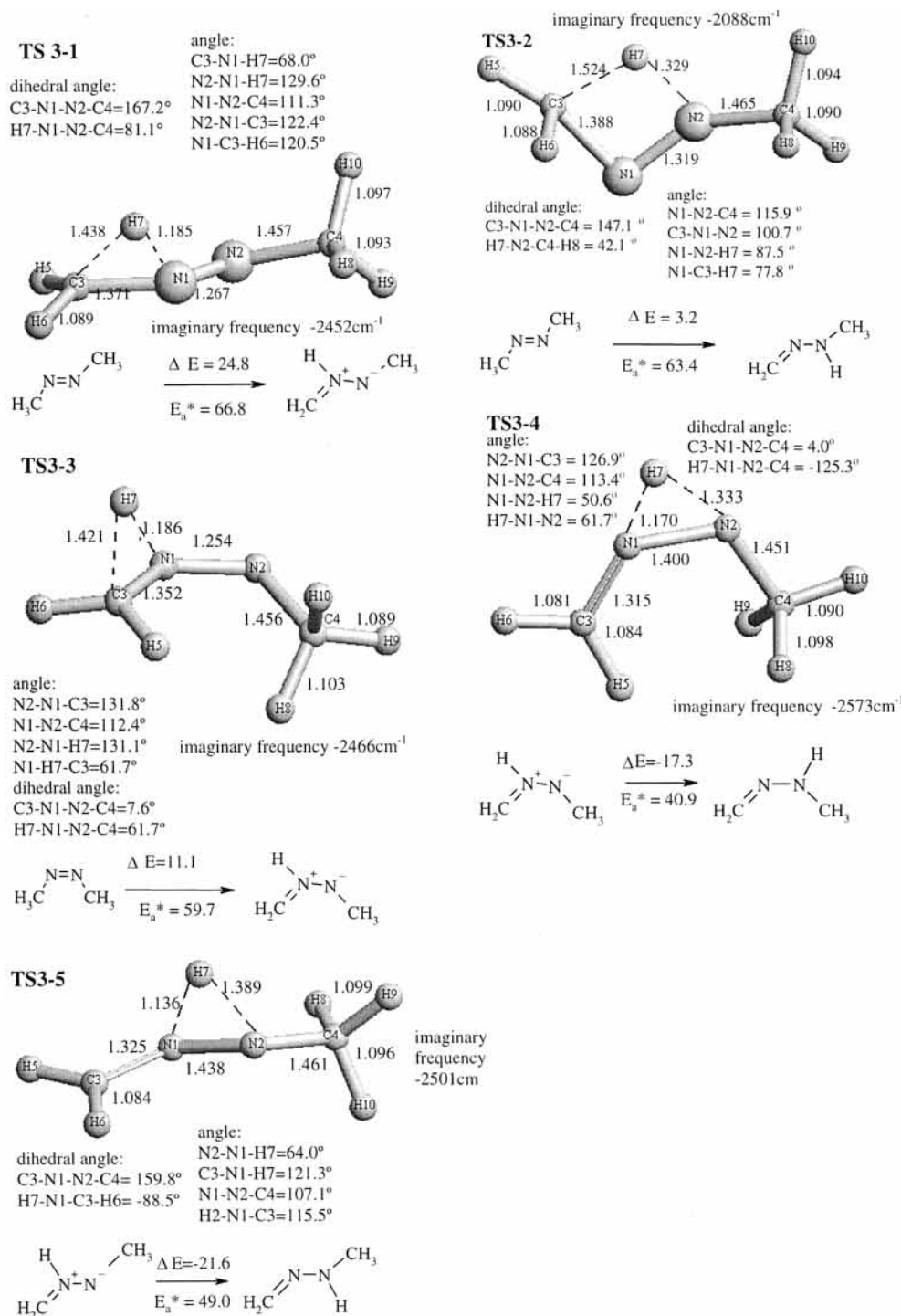


Figure 3. Transition structures at the G3 level for the hydrogen shift processes from C to N and from N to N. The unit for energy is kcal/mol, with ΔE for the energy change in a reaction and E_a^* for the reaction barrier. The bond distances are in Å.

into formaldehyde methylhydrazone (2-4) at room temperature is not substantiated by our calculations.⁵⁶ Such a reaction must go through two H migration steps, and the barrier for the first step (1,2-hydrogen shift) is 59.7 kcal/mol, accessible only by photoexcitation or at least high temperature. In fact, there is a possibility to isolate 2-1 and 2-3 experimentally in stable forms as the barriers for further hydrogen migration are more than 40 kcal/mol (Figure 3). As will be discussed later, the energy required to break the N-N bond in 2-1 and 2-3 is even higher. In addition to formaldehyde methylhydrazone (2-2 and 2-4), 2-1 and 2-3 may also be present on metal surfaces.

After hydrogen migration to nitrogen atoms, the only dissociation observed in AIMD trajectories is the N-N bond

cleavage, which has been seen quite often in the thermal dissociation of azomethane on metal surfaces.^{16,17,19,21} We thus further studied the mechanisms of N-N bond scission after 1,2- and 1,3-hydrogen shifts, as shown in Figure 4. At the unrestricted MP2/6-311G(2d,p) level, we did structure optimization for both 2-1 and 2-3 with N-N distance fixed at values gradually stretched from 1.3 to 2.9 Å. The barrier thus obtained for breaking the N-N bond is 70.5 kcal/mol for 2-1 and 76.1 kcal/mol for 2-3. As expected, both values are higher than the single bond N-N dissociation energy of 59 kcal/mol.⁵⁷ When the N-N distance was stretched beyond 2.3 Å, the CH₃N fragment went through isomerization and became H₂CNH. Previous ab initio studies^{58,59} found such a process to be

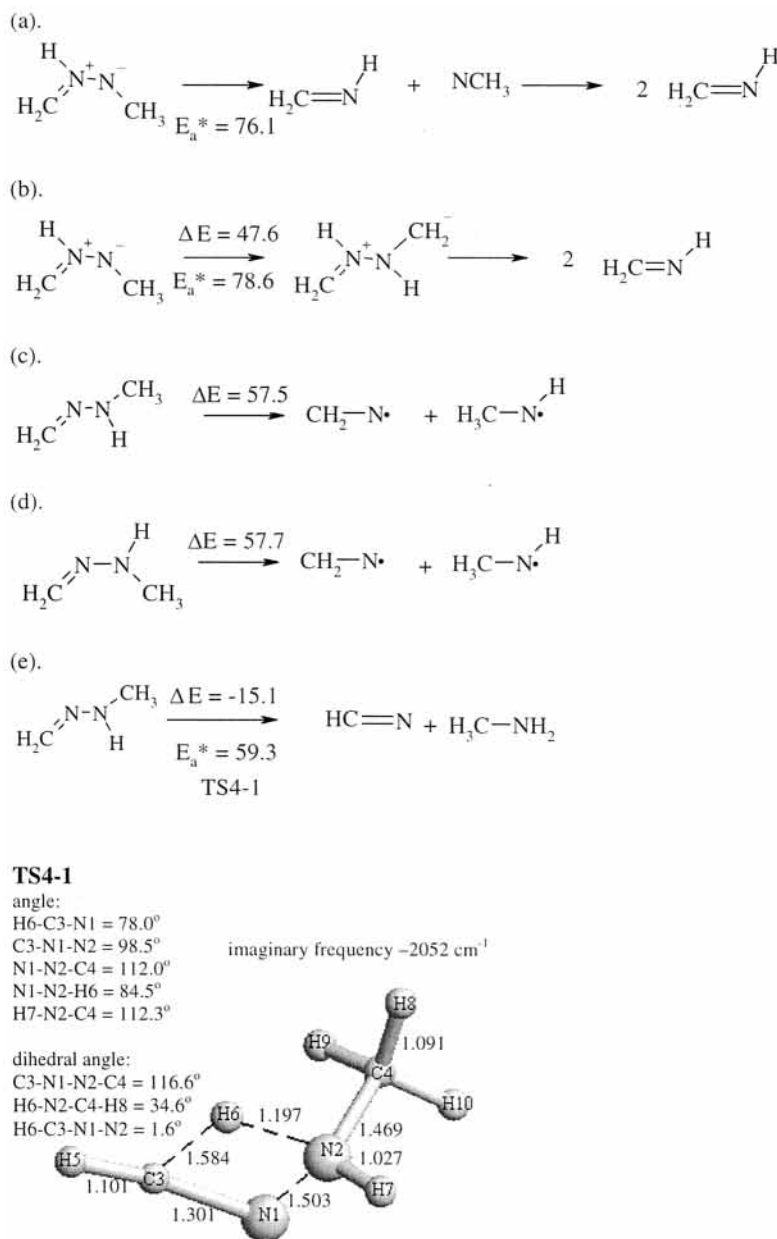


Figure 4. N–N bond cleavage for the structures shown in Figure 2. The unit for energy is kcal/mol, with ΔE for the energy change in a reaction and E_a^* for the reaction barrier. (a) Direct stretching of the N–N bond in 2–3. (b) Stretching of the N–N bond coupled with hydrogen migration for 2–3. (c) Direct stretching of the N–N bond for 2–2. (d) Direct stretching of the N–N bond for 2–4. (e) N–N cleavage for 2–2 by hydrogen migration through TS4–1, with bond distance shown in Å. The energy value for (a) is obtained at the unrestricted MP2/6-311G(2d,p) level, while all other values are obtained at the G3 level.

exothermic by more than 80 kcal/mol with a barrier just around 3 kcal/mol.⁵⁸ We thus explored the possibility of a further hydrogen migration from the methyl group to form two H_2CNH simultaneously with N–N bond cleavage. A transition structure is located for such a mechanism, but the reaction barrier at 78.6 kcal/mol is very unfavorable.

For formaldehyde methylhydrazone (2–2 and 2–4), homolysis of the N–N bond requires more than 57 kcal/mol at the G3 level, comparable to the standard N–N dissociation energy of 59 kcal/mol.⁵⁷ There is an additional channel in which one hydrogen from the methylene group goes through a further 1,3-hydrogen migration, and the molecule breaks into HCN and CH_3NH_2 . As shown in Figure 4, the barrier for such a migration at 59.3 kcal/mol is only slightly higher than that for the N–N homolysis channels, and the overall energy change is exothermic by 15.1 kcal/mol. As discussed above, the rotation around the

N–N bond in 2–2 and 2–4 is fairly free, and this dissociation channel should be accessible for both isomers.

Our results lend proof to the previous experimental conclusion that the N–N bond cleavage for azomethane on metal surfaces is preceded by the hydrogen migration from carbon to nitrogen atoms.^{16,17,19,21} There exist two distinct migration paths, 1,2- and 1,3-hydrogen shifts, while the N–N cleavage is easier following the 1,3-hydrogen shifts. The cleavage mechanism may well depend on the change in bond strengths upon adsorption of azomethane on metal surfaces. Hydrogen migration is facilitated by the weakening of the C–H bond, and further H migration in formaldehyde methylhydrazone results in a dissociation into HCN and CH_3NH_2 , both of which have been observed in previous experiments.^{16,17,19} If the strength of the N–N bond is much weakened, then the N–N cleavage is also likely to happen and the products are two radicals $\text{CH}_2\text{N}\cdot$ and

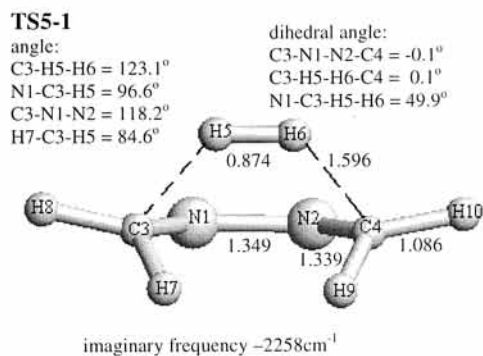
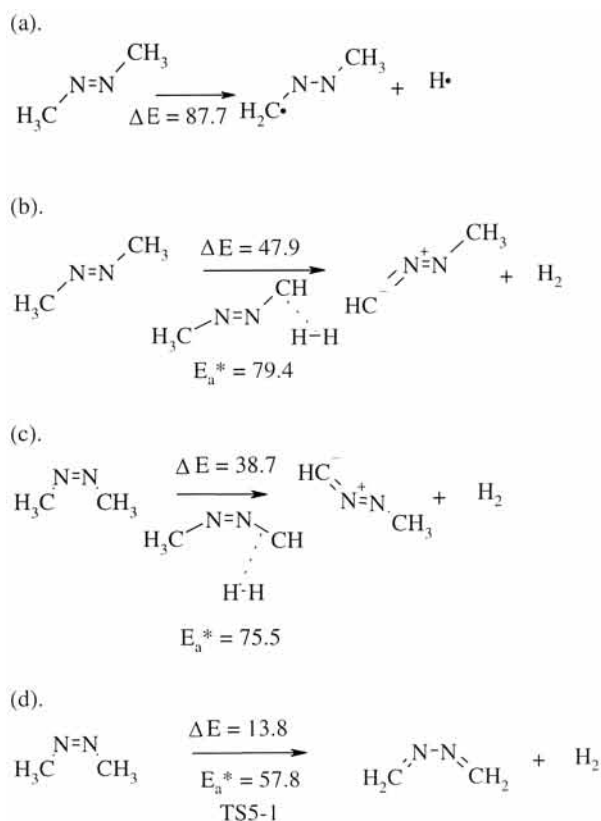


Figure 5. Hydrogen loss channels, with energy in kcal/mol, ΔE for the energy change in a reaction and E_a^* for the reaction barrier, with (a) and (d) at the G3 level and with (b) and (c) at the B3LYP/6-31G(d) level. (a) C–H bond cleavage. (b) Concerted C–H bond cleavages in one methyl group to form H_2 for *trans*-azomethane. (c) Concerted C–H bond cleavages in one methyl group to form H_2 for *cis*-azomethane. (d) Concerted C–H bond cleavages in two methyl groups to form H_2 through TS5-1, with bond distance in Å. Notice the last channel is possible only for *cis*-azomethane.

$\text{CH}_3\text{NH}\cdot$, which would probably be adsorbed on metal surface and go through further reactions upon heating. According to the electron energy loss spectral measurement of azomethane adsorbed on the Mo(110) surface,¹⁸ the C–H stretching frequency red shifted approximately 60 cm^{-1} upon surface adsorption, while the N=N stretch frequency barely moved, indicating a larger degree of weakening in the C–H bond than that in the N=N bond. In the same experiment, $\text{CH}_2=\text{NNHCH}_3$, the product of hydrogen shift, was indeed identified as the main product, in agreement with our calculations, although the situation may vary on the surfaces of different types of metal.¹⁶

Hydrogen Loss Channels. In our AIMD trajectory study, a few hydrogen loss reactions with C–H bond cleavage were also

observed. As shown in Tables 1 and 2, and Figure 5, these channels involve either the homolysis of a single C–H bond or the concerted cleavage of two C–H bonds together with the formation of H_2 . Most of these channels have very high energy barriers, above 75 kcal/mol , and are very unlikely to be present in the dissociation studies either in the gas phase or on metal surfaces. For channels (b) and (c) in Figure 5, both G3 and CASSCF(10,8) methods failed to locate the transition structures, which were found only in the B3LYP/6-31G(d) optimizations. These channels are observed in the AIMD trajectory study because a high temperature of 3500 K was used in our simulations to facilitate the observation of dissociation channels. This is similar to our previous study on acetic acid,⁴³ in which high barrier channels were also observed due to high simulation temperatures.

The one exception among these channels is the H_2 elimination channel for *cis*-azomethane, through a concerted mechanism in which one C–H bond in each of the two methyl groups is broken while H_2 is being formed, and there is a six member ring in the transition structure (TS5-1), as shown in Figure 5. The energy barrier at 57.8 kcal/mol is actually slightly lower than that for the 1,2-hydrogen shift channel for *cis*-azomethane. On the metal surfaces, if 1,2-hydrogen shift could proceed due to the weakening of C–H bond,¹⁸ this H_2 loss channel could be enhanced by the same reason. H_2 loss was observed before in the azomethane dissociation on surfaces;^{16,17} however, they were attributed to the dissociation of *trans*-azomethane, for which this mechanism cannot be applied due to geometry constraints.

Summary

By combining an AIMD trajectory study with Gaussian-based ab initio calculations, we have identified new channels in the thermal dissociation of both *cis*- and *trans*-azomethane and mapped out their corresponding reaction barriers and transition structures.

There is a methane elimination channel for *cis*-azomethane, in which the departing methyl group captures a hydrogen atom in the other methyl group. The products are CH_4 , methane, and CH_2N_2 , diazomethane, which is a well-known source of CH_2 . The reaction barrier at 47.5 kcal/mol at B3LYP/6-31G(d) level is not much higher than that for the C–N bond homolysis or the *cis*–*trans* isomerization, and thus this channel could also be present in the gas-phase dissociation, although its rate should be lower than that for the C–N homolysis.

For hydrogen migration from C to N atoms, as previously observed in the dissociation of azomethane on metal surfaces, there are actually two distinct paths for *trans*-azomethane: a 1,2-hydrogen shift to produce $\text{CH}_2=\text{NH}^+-\text{N}^-\text{CH}_3$ and a 1,3-hydrogen shift to produce $\text{CH}_2=\text{N}-\text{NHCH}_3$ (formaldehyde methylhydrazone). For *cis*-azomethane, only the 1,2-hydrogen shift is possible due to geometry constraints, but a further step of H migration is possible for the isomerization of $\text{CH}_2=\text{NH}^+-\text{N}^-\text{CH}_3$ into $\text{CH}_2=\text{N}-\text{NHCH}_3$. The observed N–N bond cleavage is likely due to formaldehyde methylhydrazone, $\text{CH}_2=\text{N}-\text{NHCH}_3$. If C–H bond is weakened upon adsorption on a metal surface, a further step of hydrogen migration from the methylene group would break the N–N bond and produce HCN and CH_3NH_2 , both found in previous surface experiments. If N–N bond is weakened on metal surface, the homolysis of N–N bond would produce two radicals, $\text{CH}_2\text{N}\cdot$ and $\text{CH}_3\text{NH}\cdot$.

The H or H_2 loss channels have reaction barriers higher than 75 kcal/mol , and they are unlikely to occur either in gas phase or on metal surfaces. The only exception is for *cis*-azomethane,

in a mechanism with the cleavage of a C–H bond in one methyl group concerted with another C–H cleavage in the second methyl group. The barrier for such a process is actually slightly lower than the 1,2-hydrogen shift for *cis*-azomethane.

Acknowledgment. We thank Mr. Bing-wu Wang for his assistance with the RRKM calculations. The work reported is supported by an Earmarked Grant (Project No. CUHK 4188/97P) from the Research Grants Council of Hong Kong SAR Government. We are grateful to the generous allocation of computer time on the clusters of AlphaStations at the Chemistry Department and on the Origin 2000 at the Information Technology Service Center, both at the Chinese University of Hong Kong (CUHK). We also thank Mr. Frank Ng and Mr. Ka Fai Woo for technical support.

Supporting Information Available: Atomic coordinates for all the transition and intermediate structures shown in Figures 1–5; RRKM calculation results for the stepwise C–N homolysis and CH₄ elimination channels. This material is available free of charge via the Internet at <http://pubs.acs.org>.

References and Notes

- (1) Ramsperger, H. C. *J. Am. Chem. Soc.* **1927**, *49*, 912.
- (2) Engel, P. S. *Chem. Rev.* **1980**, *80*, 99.
- (3) Andrews, B. K.; Burton, K. A.; Weisman, R. B. *J. Chem. Phys.* **1992**, *96*, 1111.
- (4) Burton, K. A.; Weisman, R. B. *J. Am. Chem. Soc.* **1990**, *112*, 1804.
- (5) Fairbrother, D. H.; Dickens, I. M.; Stair, P. C.; Weitz E. *Chem. Phys. Lett.* **21995**, *46*, 513.
- (6) North, S. W.; Longfellow, C. A.; Lee, Y. T. *J. Chem. Phys.* **1993**, *99*, 4423.
- (7) Diau, E. W.-G.; Abou-Zied, O. K.; Scala, A. A.; Zewail, A. H. *J. Am. Chem. Soc.* **1998**, *120*, 3245.
- (8) Bracker, A. S.; North, S. W.; Suits, A. G.; Lee, Y. T. *J. Chem. Phys.* **1998**, *19*, 7238.
- (9) Gejo, T.; Felder, P.; Huber, J. R. *Chem. Phys.* **1995**, *195*, 423.
- (10) Liu, R.; Cui, Q.; Dunn, K. M.; Morokuma, K. *J. Chem. Phys.* **1996**, *15*, 2333.
- (11) Hu, C. H.; Schaefer, H. F., III *J. Phys. Chem.* **1995**, *99*, 7505.
- (12) Hu, C. H.; Schaefer, H. F., III *J. Chem. Phys.* **1994**, *11*, 1289.
- (13) Andrews, B. K.; Weisman, R. B. *J. Chem. Phys.* **1994**, *11*, 6776.
- (14) Cattaneo, P.; Persico, M. *Chem. Phys. Lett.* **1998**, *289*, 160.
- (15) Cattaneo, P.; Persico, M. *Theor. Chem. Acc.* **2000**, *103*, 390.
- (16) Kiss, A.; Barthos, R.; Kiss, J. *Phys. Chem. Chem. Phys.* **2000**, *2*, 4237.
- (17) Bol, C. W. J.; Kovacs, J. D.; Chen, M.; Friend, C. M. *J. Phys. Chem. B* **1997**, *101*, 6436.
- (18) Weldon, M. K.; Friend, C. M. *Surf. Sci.* **1994**, *310*, 95.
- (19) Jentz, D.; Trenary, M.; Peng, X. D.; Stair, P. *Surf. Sci.* **1995**, *341*, 282.
- (20) Castro, M. E.; Pressley, L. A.; White, J. M. *Surf. Sci.* **1991**, *256*, 227.
- (21) Hanley, L.; Guo, X. C.; Yates, J. T., Jr. *J. Phys. Chem.* **1989**, *93*, 6754.
- (22) Camp, R. N.; Epstein, I. R.; Steel, C. *J. Am. Chem. Soc.* **1977**, *99*, 2453.
- (23) Dannenberg, J. J.; Rocklin, D. *J. Org. Chem.* **1982**, *47*, 4529.
- (24) Howell, J. M.; Kirschenbaum, L. J. *J. Am. Chem. Soc.* **1976**, *8*, 877.
- (25) Vrábel, I.; Biskupič, S.; Staško, A. *J. Phys. Chem. A* **1997**, *101*, 5805.
- (26) Vrábel, I.; Biskupič, S.; Staško, A. *Theor. Chim. Acta* **1997**, *95*, 201.
- (27) Kresse, G.; Furthmüller, J. *Phys. Rev. B* **1996**, *54*, 11169.
- (28) Kresse, G.; Hafner, J. *Phys. Rev. B* **1993**, *47*, 558.
- (29) Kresse, G.; Hafner, J. *Phys. Rev. B* **1991**, *49*, 14251.
- (30) Kresse, G.; Furthmüller, J. *Comput. Mater. Sci.* **1996**, *6*, 15.
- (31) Car, R.; Parrinello, M. *Phys. Rev. Lett.* **1985**, *55*, 2471.
- (32) Parrinello, M. *Solid State Commun.* **1997**, *12*, 107.
- (33) Remler, D. K.; Madden, P. A. *Mol. Phys.* **1990**, *70*, 921.
- (34) Payne, M. C.; Teter, M. P.; Allan, D. C.; Arias, T. A.; Joannopoulos, J. D. *Rev. Mod. Phys.* **1992**, *64*, 1045.
- (35) Tuckerman, M. E.; Ungar, P. J.; Vonrosenvinge, T.; Klein, M. L. *J. Phys. Chem.* **1996**, *10*, 12878.
- (36) Perdew, J. P. In *Electronic Structure of Solids '91*; Ziesche, P., Eschrig, H., Eds.; Akademie Verlag: Berlin, 1991; p 11.
- (37) Vanderbilt, D. *Phys. Rev. B* **1990**, *41*, 7892.
- (38) Kresse, G.; Hafner, J. *J. Phys. Condens. Matter* **1994**, *6*, 8245.
- (39) Kresse, G.; Hafner, J. *Phys. Rev. B* **1993**, *48*, 13115.
- (40) Nosé, S. *J. Chem. Phys.* **1984**, *81*, 511.
- (41) Hoover, W. G. *Phys. Rev. A* **1985**, *31*, 1695.
- (42) Yim, Y. W.; Liu, Z. F. *J. Am. Chem. Soc.* **2001**, *123*, 2243.
- (43) Liu, Z. F.; Siu, C. K.; Tse, J. S. *Chem. Phys. Lett.* **1999**, *314*, 317.
- (44) Curtiss, L. A.; Raghavachari, K.; Redfern, P. C.; Rassolov, V.; Pople, J. A. *J. Chem. Phys.* **1998**, *19*, 7764.
- (45) Baboul, A. G.; Curtiss, L. A.; Redfern, P. C.; Raghavachari, K. *J. Chem. Phys.* **1999**, *110*, 7650.
- (46) Frisch, M. J.; Trucks, G. W.; Schlegel, H. B.; Scuseria, G. E.; Robb, M. A.; Cheeseman, J. R.; Zakrzewski, V. G.; J. A. Montgomery, J.; Stratmann, R. E.; Burant, J. C.; Dapprich, S.; Millam, J. M.; Daniels, A. D.; Kudin, K. N.; Strain, M. C.; Farkas, O.; J. Tomasi; Barone, V.; Cossi, M.; Cammi, R.; Mennucci, B.; Pomelli, C.; Adamo, C.; Clifford, S.; Ochterski, J.; Petersson, G. A.; Ayala, P. Y.; Q. Cui; Morokuma, K.; Malick, D. K.; Rabuck, A. D.; Raghavachari, K.; Foresman, J. B.; Cioslowski, J.; Ortiz, J. V.; Baboul, A. G.; Stefanov, B. B.; Liu, G.; Liashenko, A.; Piskorz, P.; Komaromi, I.; Gomperts, R.; Martin, R. L.; Fox, D. J.; Keith, T.; Al-Laham, M. A.; Peng, C. Y.; Nanayakkara, A.; Gonzalez, C.; Challacombe, M.; Gill, P. M. W.; Johnson, B.; Chen, W.; Wong, M. W.; Andres, J. L.; Gonzalez, C.; Head-Gordon, M.; Replogle, E. S., J. A. Pople *Gaussian 98*; Gaussian, Inc.: Pittsburgh, PA, 1998.
- (47) Goldstein, E.; Beno, B.; Houk, K. N. *J. Am. Chem. Soc.* **1996**, *118*, 6036.
- (48) Almenningen, A.; Anfinsen, I. M.; Haaland, A. *Acta Chem. Scand.* **1970**, *24*, 1230.
- (49) Longfellow, C. A.; Lee, Y. T. *J. Phys. Chem.* **1995**, *99*, 15532.
- (50) Nguyen, M. T.; Sengupta, D.; Raspoet, G.; Vanquickenborne, L. G. *J. Phys. Chem.* **1995**, *99*, 11883.
- (51) Duan, X.; Page, M. *J. Am. Chem. Soc.* **1995**, *117*, 5114.
- (52) Gilbert, R. G.; Smith, S. C. *Theory of Unimolecular and Recombination Reactions*; Blackwell Scientific Publications: Oxford, 1990. Gilbert, R. G.; Smith, S. C.; Jordan, M. J. T. *UNIMOL program suite* (calculation of falloff curves for unimolecular and recombination reactions), 1993. Available from the authors: School of Chemistry, Sydney University, NSW 2006, Australia.
- (53) The RRKM was performed using the UNIMOL program. The assumed pressure is 1 atm. Results of calculation at temperatures ranging from 500 to 3500 K are provided in the Supporting Information.
- (54) Lemal, D. M.; Menger, F.; Coats, E. *J. Am. Chem. Soc.* **1964**, *86*, 2395.
- (55) McKee, M. L. *J. Am. Chem. Soc.* **1990**, *112*, 7957.
- (56) Ackermann, M. N.; Craig, N. C.; Isberg, R. R.; Lauter, D. M.; MacPhail, R. A.; Young, W. G. *J. Am. Chem. Soc.* **1977**, *99*, 1661.
- (57) Huheey, J. E.; Keiter, E. A.; Keiter, R. L. *Inorganic Chemistry: principles of structure and reactivity*, 4th ed.; HarperCollins College Publishers: New York, 1993.
- (58) Kemnitz, C. R.; Ellison, G. B.; Karney, W. L.; Borden, W. T. *J. Am. Chem. Soc.* **2000**, *122*, 1098.
- (59) Richards, C., Jr.; Meredith, C.; Kim, S. J.; Quelch, G. E.; Schaefer, H. F., III *J. Chem. Phys.* **1994**, *10*, 481.